# Blunted neural and psychological stress processing predicts future grey matter atrophy in multiple sclerosis

Lil Meyer-Arndt [a], Stefan Hetzer [b], Susanna Asseyer [a], Judith Bellmann-Strobl [a,c], Michael Scheel [a], Jan-Patrick Stellmann [d,e,f], Christoph Heesen [d], Andreas K. Engel [g], Alexander U. Brandt [a,l], John-Dylan Haynes [a,b,h], Friedemann Paul [a,c,i,1], Stefan M. Gold [d,j,k,1], Martin Weygandt [a,b,*,1]

[a] Charité – Universitätsmedizin Berlin, Corporate Member of Freie Universität Berlin, Humboldt-Universität zu Berlin, And Berlin Institute of Health, NeuroCure Clinical Research Center, 10117, Berlin, Germany
[b] Charité – Universitätsmedizin Berlin, Corporate Member of Freie Universität Berlin, Humboldt-Universität zu Berlin, And Berlin Institute of Health, Berlin Center for Advanced Neuroimaging, 10117, Berlin, Germany
[c] Max Delbrück Center for Molecular Medicine and Charité – Universitätsmedizin Berlin, Corporate Member of Freie Universität Berlin, Humboldt-Universität zu Berlin, And Berlin Institute of Health, Experimental and Clinical Research Center, 13125, Berlin, Germany
[d] Institute of Neuroimmunology and Multiple Sclerosis (INIMS), Center for Molecular Neurobiology Hamburg, University Medical Center Hamburg-Eppendorf, 20251, Hamburg, Germany
[e] Aix-Marseille Univ, CNRS, CRMBM, UMR, 7339, Marseille Cedex, France
[f] APHM, Hopital de la Timone, CEMEREM, Marseille, France
[g] Department of Neurophysiology and Pathophysiology, University Medical Center Hamburg-Eppendorf, 20246, Hamburg, Germany
[h] Charité – Universitätsmedizin Berlin, Corporate Member of Freie Universität Berlin, Humboldt-Universität zu Berlin, Berlin Institute of Health, Bernstein Center for Computational Neuroscience, 10117, Berlin, Germany
[i] Charité – Universitätsmedizin Berlin, Corporate Member of Freie Universität Berlin, Humboldt-Universität zu Berlin, And Berlin Institute of Health, Department of Neurology, 10117, Berlin, Germany
[j] Charité – Universitätsmedizin Berlin, Corporate Member of Freie Universität Berlin, Humboldt-Universität zu Berlin and Berlin Institute of Health, Department of Psychiatry and Psychotherapy, Campus Benjamin Franklin, 12203, Berlin, Germany
[k] Charité – Universitätsmedizin Berlin, Corporate Member of Freie Universität Berlin, Humboldt-Universität zu Berlin, And Berlin Institute of Health, Department of Psychosomatic Medicine, 10117, Berlin, Germany
[l] Department of Neurology, University of California, Irvine, CA, USA

## ARTICLE INFO

## ABSTRACT

Background: Multiple sclerosis (MS) is characterized by two neuropathological key aspects: inflammation and neurodegeneration. Clinical studies support a prospective link between psychological stress and subsequent inflammatory disease activity. However, it is unknown if a similar link exists for grey matter (GM) degeneration as the key driver of irreversible disability.

Methods: We tested whether neural network activity triggered in a psychological fMRI stress paradigm (a mental arithmetic task including social evaluation) conducted at a baseline time point predicts future GM atrophy in 25 persons with MS (14 females). Atrophy was determined between the baseline and a follow-up time point with a median delay of 1012 (Rg: 717–1439) days. Additionally, atrophy was assessed in 22 healthy subjects (13 females; median delay 771 [Rg: 740–908] days between baseline and follow-up) for comparison.

Results: An analysis of longitudinal atrophy in patients revealed GM loss in frontal, parietal, and cerebellar areas. Cerebellar atrophy was more pronounced in patients than controls. Future parietal and cerebellar atrophy could be predicted based on activity of two networks. Perceived psychological stress was negatively related to future parietal atrophy in patients and activity of the network predictive of parietal atrophy was positively linked to perceived stress.

Conclusions: We have shown that blunted neural and psychological stress processing have a detrimental effect on the course of MS and are interrelated. Together with research showing that psychological and neural stress

---

* Corresponding author. Charité – Universitätsmedizin Berlin, Charitéplatz 1, 10117, Berlin, Germany.
  E-mail address: martin.weygandt@charite.de (M. Weygandt).
[1] These authors contributed equally to this work.

processing can be altered through interventions, our findings suggest that stress processing might constitute an important modifiable disease factor.

## 1. Introduction

Multiple sclerosis (MS) is a demyelinating autoimmune disorder of the central nervous system characterized by an inflammatory and neurodegenerative component (Reich et al., 2018). The clinical phenotype can comprise sensorimotor, cognitive and neuropsychiatric symptoms such as depression and fatigue (Compston and Coles, 2008).

Consistently, a role of psychological stress in the pathobiology of the disease has been assumed since the first description of MS by Charcot (1877) and this assumption is now supported by epidemiological and clinical studies. A Swedish cohort study including 106,464 persons with stress-related disorders (e.g., Post-Traumatic Stress Disorder) and 1,064,640 without showed that these disorders increase the risk for later development of autoimmune disorders including MS (Song et al., 2018). Prospective clinical studies found an association between stressful events and subsequent symptom exacerbation, relapses and inflammatory activity (Mohr et al., 2004; Golan et al., 2008). Finally, alleviation of stress has a buffering effect on MS activity as participation in stress-management programs reduced the risk of developing new MRI lesions in a randomized controlled trial (Mohr et al., 2012).

Despite these clinico-epidemiological findings, not much is known about the biological mechanisms connecting psychological stress and MS. Specifically, although pharmacological challenge studies including our own have revealed associations between peripheral stress systems and disease activity, the role of psychological stress for this association was not addressed by this work (Gold et al., 2005; Kern et al., 2013). Moreover, although we could show in a cross-sectional neuroimaging study employing a stress paradigm (Weygandt et al., 2016) that insular activity reflects the clinical disability of persons with MS (pwMS) and that activity in overlapping cerebellar regions of pwMS and healthy controls (HCs) was linked to grey matter (GM) fraction in both groups, this study did not clarify the role of neurocognitive stress processing for future GM degeneration.

Evaluating this role, however, might be crucial as i. GM atrophy is the main driver of irreversible disability progression in MS (Confavreux and Vukusic, 2006; Geurts et al., 2012; Eshaghi et al., 2018), ii. no convincing pharmacological treatment currently exists to halt GM atrophy (Kalincik, 2017), and iii. neural stress processing is modifiable through cognitive interventions (Sinha et al., 2016). To test a link between stress and future GM atrophy in MS, we thus investigated whether neural network activity triggered by a stress paradigm (i.e., a mental arithmetic task comprising social evaluation and ratings of perceived stress) conducted at a baseline time point ('T0') predicts GM atrophy accumulated between baseline and a follow-up time point ('T1') roughly 1000 days later. Specifically, we tested the hypotheses that perceived psychological and neural network stress responses predict the degree of longitudinal GM volume loss in each region subject to atrophy in patients. Moreover, we tested the hypotheses that each neural network significantly predicting longitudinal GM atrophy is significantly related to perceived psychological stress.

## 2. Materials and methods

### 2.1. Participants

The present study is a longitudinal extension of our cross-sectional study (Weygandt et al., 2016) from which the baseline (T0) pwMS data (i.e., anatomical and functional MRI, heart rate, perceived stress, and salivary cortisol) and T0 fMRI stress data of a group of 21 HCs (referred to as 'fMRI control group' in the following) were taken. To gather follow-up anatomical MRI scans, all pwMS participating in

Weygandt et al. (2016) were re-invited in the present study for a follow-up visit (T1). Twenty-six of the 36 pwMS measured at baseline agreed to participate. All scans were acquired at the Berlin Center for Advanced Neuroimaging at Charité – Universitätsmedizin Berlin. The inclusion criteria at T1 comprised i. a diagnosis of relapsing-remitting or secondary progressive MS according to the McDonald Criteria 2017 (Thompson et al., 2017), ii. stable disease-modifying treatment for at least six months or no disease-modifying treatment, iii. no neurologic diseases other than MS and iv. age ≥18 years. Exclusion criteria were: Pregnancy, mental or addictive disorders, neurologic diseases other than MS, acute MS relapses or infections, MRI contraindications and poor MRI image quality. The visual inspection of anatomical MRI scans revealed low data quality for one patient. Other criteria did not apply. Experienced neurologists examined and diagnosed all participating patients. Clinical disability was assessed using the Expanded Disability Status Scale (EDSS; Kurtzke, 1983). Participants' study visits were approved by the research ethics committee of Charité – Universitätsmedizin Berlin (EA1/182/10, amendment V).

Additionally, we analyzed longitudinal structural MRI (sMRI) data from a group of 22 other HCs (not yet presented elsewhere and referred to as 'sMRI control group') which were originally obtained in a natural history cohort from the University Medical Center Hamburg-Eppendorf in Hamburg including clinical and MRI visits at baseline (T0) and at around 24 months (T1). The inclusion criteria were i. an age between 18 and 65, ii. no evidence of medical illness or substance abuse that may affect cognitive functioning, and iii. no psychiatric or neurological diseases (based on medical history and physical exam). Exclusion criteria were MRI contraindications and poor MRI image quality. As no exclusion criteria applied, all 22 HCs were included. Study visits in Hamburg were approved by the ethics committee of the Hamburg Medical Association (PV4356). Written consent was obtained from all participants according to the Declaration of Helsinki.

### 2.2. Experimental stress paradigm

The fMRI stress task is delineated in Fig. 1.

### 2.3. MRI sequences

MR images of pwMS at T0 and T1 and of the 21 HCs from the fMRI control group at T0 were acquired with a 3 T whole-body tomograph (Magnetom Trio, Siemens, Erlangen, Germany) using a standard 12-channel head coil. To acquire fMRI scans, we used a pseudo-continuous Arterial-Spin Labeling (ASL) Echo-Planar Imaging (EPI) sequence (Wang et al., 2005). In addition, two spin-echo EPI reference volumes with opposite phase encoding directions (anterior to posterior, posterior to anterior) were acquired in advance to the Rest and Stress fMRI measurements to facilitate $B_0$-unwarping of fMRI images. Anatomical images were acquired with T1-weighted and T2-weighted sequences. Anatomical T1-weighted MRI scans of the HCs from the sMRI control group were acquired with a 3 T whole-body tomograph (Magnetom Skyra, Siemens, Erlangen, Germany) and a standard 32-channel head coil. See supplementary methods for details.

### 2.4. MRI preprocessing

#### 2.4.1. Anatomical images

Preprocessing of anatomical MRI data comprised i. a manual lesion mapping procedure, ii. segmentation of T1-weighted anatomical images, iii. determination of a GM group mask for fMRI analyses, and iv. a determination of the volume of 122 GM regions defined by a

neuroanatomical atlas for T0 and T1. In the latter step, the volume of each individual region, participant, and both time points was computed based on the spatial brain segmentation procedure that enables allocation of intracranial voxel coordinates to one of three tissue classes: GM, white matter, and cerebrospinal fluid. After the number of GM voxels was determined for each atlas region, we computed the regional GM volume by multiplying the number of voxels by the volume of a voxel in $mm^3$. Regional volume data were then entered as criteria into our group MRI analysis. Please see supplementary methods for details.

### 2.4.2. Functional images

In this study, we evaluated fMRI images that were already analyzed in Weygandt et al. (2016). Preprocessing of these images comprised six steps, i.e., i. co-registration of perfusion fMRI scans to spin-echo EPI volumes acquired for $B_0$-unwarping, ii. $B_0$-unwarping of fMRI scans, iii. coregistration of fMRI scans to anatomical T1-weighted scans, iv. spatial smoothing of fMRI scans, v. computation of voxel images assessing the average cerebral blood flow (CBF; ml/100 g/min) for the (final) 8 min of the Rest and the Stress measurement based on control-label pairs. Finally, in step vi. we used the mapping parameters computed during segmentation of T1-weighted scans to register the average CBF maps of both fMRI conditions to the MNI standard space. These spatially normalized CBF maps (voxel size of $3 \cdot 3 \cdot 3\ mm^3$) computed for each patient and both fMRI conditions separately entered the fMRI group

analysis. See supplementary methods for details.

### 2.5. Statistical analyses

#### 2.5.1. Longitudinal GM atrophy

We conducted two subanalyses to evaluate longitudinal atrophy in pwMS (and HCs of the sMRI control group) in 2.5.1. The main goal of 2.5.1, which was addressed in the first subanalysis, was to identify GM areas (among 122 regions included in the neuroanatomical atlas) that were characterized by longitudinal volume loss in the period from T0 to T1 in MS patients (i.e., areas showing a main effect of time in pwMS). In the second subanalysis, conducted to clarify whether volume loss of areas putatively found in the first subanalysis was specific for MS, we evaluated in which of these regions the impact of time on volume loss differed between patients and controls (interaction effect of time and group). In both analyses, linear-mixed effects (LME) regression (cf. Weygandt et al., 2019) was applied using the FITLMEMATRIX algorithm implemented in Matlab (2014a) (MathWorks, Natick, Massachusetts, USA) to evaluate longitudinal effects.

In the first analysis, the regressor of interest coded zeros for the T0 measurement and the number of days after T0 for T1. Sex, age, progressive MS (y/n), and a fixed and random intercept were modelled as covariates of no interest. We report regions with GM volume reductions significant according to a Family-Wise Error (FWE)-corrected threshold
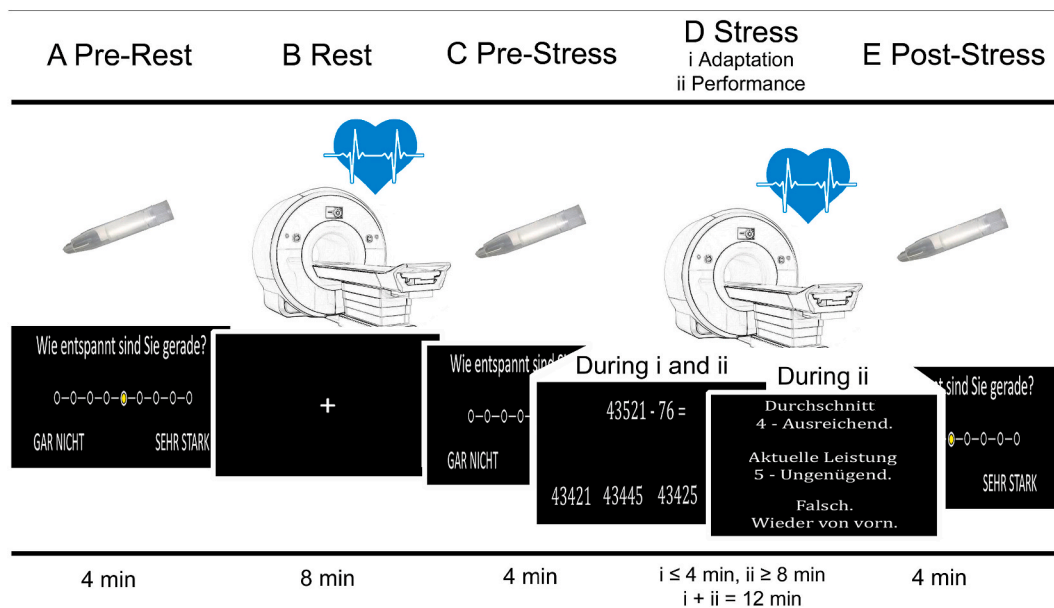


**Fig. 1. Mental arithmetic stress paradigm** which was derived from Wang et al. (2005). In the first of five stages evaluated in this study ('A Pre-Rest'), participants rated the experienced degree of distress, relaxation, frustration, and anxiety on a 9-point self-report scale presented on a projection screen inside the scanner with MRI-compatible button boxes. Options ranged from 'Gar nicht' ('not at all') depicted at the leftmost position of the scale to 'Sehr stark' ('very strong') depicted on the rightmost position. In the second stage ('B Rest'), we conducted a baseline ASL fMRI scan during which the participants were instructed to focus on a fixation cross. Following a second self-report ('C Pre-Stress'), we conducted the main fMRI stress measurement ('D Stress'). During this stage, participants were asked to perform a series of subtraction tasks, i.e. 'operand X minus operand Y'. In each trial, a participant had to select the correct result from four numbers depicted below operands X and Y. The start value for X was 43 521 across all participants. Operand Y was randomly determined in each trial and ranged from 1 to 99. The stress block was divided in two sub-stages, an adaptation stage D(i; ≤ 4 min duration) and a performance stage D(ii; lasting for the remaining time of the total 12 min duration of D). In D(i), participants had 8 s per trial to choose a result and response times were recorded. In the case of a correct result, the difference X minus Y was used as operand X in the next trial. Otherwise, operand X remained unchanged. When 10 correct answers were given or when the 4-min. adaption stage was over, D(i) ended and D(ii) began without announcement. D(ii) differed from D(i) in three important aspects. Firstly, the time provided for each trial was adjusted based on arithmetic performance (i.e. starting at 8 s, which was decreased or increased by ten percent depending on response accuracy in preceding trials). Secondly, we provided feedback by means of school grades ranging from '1 – Sehr gut' ('very good') down to '5 – Ungenügend' ('insufficient') depending on response time for correct trials during the adaptation stage. Finally, participants had to start over again with X = 43 521 in case of false or too slow answers. After the stress block, participants rated their perceived stress level for a third time ('E Post-Stress'). We measured heart rate with a pulse oximeter (see Supplement for details) during both fMRI blocks (B, D) and computed the task load as the average duration of inter-trial intervals during the last 8 min of stage D. Task load served as covariate of no interest for statistical group analyses. Moreover, salivary cortisol was measured during all three rating stages (A, C, and E; see Supplement for details). Prior to the start of the MRI session, patients were informed about their participation in a mental arithmetic task and the feedback they would receive comparing their performance to performance parameters established in the general population. After the experiment, we explained to them that feedback was generated based on their arithmetic performance in the adaptation stage. The figure was adapted from Weygandt et al. (2016).

($\alpha_{FWE} = 0.05$) for two-sided tests computed by dividing the false positive rate for a single test of 0.05 by the number of regions in the atlas.

In the second (factorial) analysis, the interaction regressor testing the disease-specificity of the temporal dynamic of regional volume loss was computed as the element-wise product of the two main effect regressors of group and time. Both main effect regressors, sex, age, and fixed and random intercepts were included in the LME model as covariates of no interest. Again, we applied an FWE-corrected significance threshold for two-sided tests (i.e. 0.05 divided by the number of regions with significant GM loss in patients). The false positive rate of effects of interest in both LME analyses (and all other statistical tests conducted in this work) was evaluated with permutation testing (10 000 permutations of the regressor of interest; cf. [20]). Compared with parametric procedures, permutation techniques are much more robust as they do not rely on the fulfilment of distributional assumptions (Good, 2005). Please note that we report results obtained in the second/interaction analysis for the main effect of group on regional GM volume in all 122 areas in the Supplement to highlight areas affected by MS atrophy independent of the temporal dynamics of this process.

### 2.5.2. Predicting future GM atrophy in MS based on perceived stress

The main effect of perceived psychological stress on longitudinal atrophy in areas with significant atrophy in pwMS as revealed by the above analysis was tested with robust linear regression (using a bisquare M-estimator) implemented in the ROBUSTFIT Matlab 2014a algorithm. Robust regression using bisquare M-estimators is much less affected by outliers than standard (i.e., ordinary least square) regression and has consistently been proven to increase the power of statistical tests (Wager et al., 2005; Fox and Weisberg, 2019). The time between T0 and T1 in days, sex, age, task load, the presence of progressive MS (y/n), and GM volume of the respective region at T0 served as covariates of no interest (in the framework of this study). We hypothesized that perceived psychological stress predicts the degree of longitudinal GM volume loss in each GM region subject to longitudinal atrophy in patients. Each of these individual hypotheses was tested with a significance threshold of $\alpha = 0.05$ for two-sided tests. Permutation testing was used for inference (10 000 permutations).

An analysis of psychophysiological stress task responses evaluating the basic suitability of our mental arithmetic task to induce stress in terms of perceived stress, heart rate, and salivary cortisol can be found in the Supplement.

### 2.5.3. Predicting future GM atrophy in MS based on neural stress responses

Here, we tested whether we can use task-induced activity changes of neural networks to predict the longitudinal volume variations of GM areas subject to atrophy in pwMS. For this purpose, we determined neural networks composed by brain regions whose activity was strongly correlated across pwMS during the stress stage. Specifically, we first computed the average CBF for each pwMS and each GM region contained in the atlas for the resting and stress stage separately. Then, we removed each patient's overall signal mean of a given task stage from each regions' task stage mean signal ('centering'). Next, we used Singular Value Decomposition (SVD) to compute a small set of 25 hidden variables (Principal Components; PCs; see e.g., 24, 25) that reflect the shared characteristic variation underlying the signals of individual GM regions contributing to a given network during the stress stage across pwMS. Each of these hidden variables represents one network and encodes the activity of the given network for a patient as a single number. In the next step, we used the centered regional activity signals of the resting stage to determine these hidden variables as activity markers of the networks during rest. Finally, we subtracted the network activity scores computed for the resting from those of the stress stage to determine stress-induced activity changes for each pwMS. For further details (including information on the permutation-based determination of GM atlas regions contributing significantly to the different networks), see supplementary methods.

After neural network activity parameters were determined, we entered the differential stress processing markers as covariates of interest into robust regression models for the prediction of future GM volume loss. Time between T0 and T1 in days, sex, age, the presence of progressive MS (y/n), task load, GM volume of the respective region at T0 were included in the model as covariates of no interest. For each of the five GM areas subject to atrophy in patients, we computed one robust regression model for the differential stress responses of each of the 25 networks. In line with our hypotheses that the degree of longitudinal atrophy of each of the five GM areas subject to atrophy in patients can be predicted by neural network stress responses, we accounted for multiple tests by applying an FWE-corrected significance threshold for two-sided tests computed as the false positive rate of a single test (0.05) divided by the number of PCs determined. Again, permutation testing was used for inference (10 000 permutations).

An analysis of stress network activity differences between the pwMS and participants in the fMRI control group as well as an analysis testing whether future atrophy in pwMS can be predicted based on stress-related cortisol release can be found in the Supplement.

### 2.5.4. Perceived stress and neural stress responses in MS

We tested the hypotheses that each neural network whose differential stress response predicts future atrophy in patients also predicts the perceived stress ratings (i.e., post-minus pre-stress). For this purpose, one robust regression model was computed for the activity of each network fulfilling this criterion as covariate of interest. Sex, age, the presence of progressive MS (y/n), and task load were included as covariates of no interest. We applied an FWE-corrected threshold for two-sided tests (i.e., 0.05 divided by the number of atrophy-predictive networks). Permutation testing (10 000 permutations) was used for inference.

Finally, an analysis testing whether stress-related cortisol release is associated to atrophy-predictive neural network activity and perceived stress can be found in the Supplement.

## 3. Results

### 3.1. Demographic and clinical participant characteristics

Twenty-five persons with (19 relapsing-remitting; 6 secondary progressive) MS were included in the study, 22 in the sMRI control group, and 21 HCs in the fMRI control group. At T0, 18 patients received a disease modifying treatment (4 fumarate, 5 β-interferons, 4 glatiramer acetate, 4 fingolimod, and 1 teriflunomide). The median disease duration in patients at T0 relative to the onset of first symptoms was 9.72 (Rg = 1.30–33.54) years. The median clinical-severity assessed with the EDSS (Kurtzke, 1983) was 3.5 at both visits (T0: Rg = 1–6; T1: Rg = 0–6). See Table 1 below and supplementary results for further demographic and clinical participant characteristics.

**Table 1**
Demographic and clinical participant characteristics. False positive rate of test statistics was computed with permutation testing (10 000 permutations). Abbreviations: HSD – high school diploma.

| Group | Sex (f/m) | Age (yrs) | HSD(y/n) | Follow-up interval (days) |
|---|---|---|---|---|
| | # | MD RG | # | MD RG |
| MS | 14/11 | 50 27–62 | 15/10 | 1012 717–1439 |
| HC - sMRI | 13/9 | 44 30–57 | 13/9 | 771 740 - 908 |
| HC - fMRI | 13/8 | 51 25–64 | 16/5 | |
| | $\chi^2$ p | t p | $\chi^2$ p | t p |
| MS vs. HC - sMRI | 0.05 > 0.999 | 2.41 0.021 | 0.00 > 0.999 | $6.92 < 10^{-4}$ |
| MS vs. HC - fMRI | 0.160.765 | −0.10 0.926 | 1.36 0.344 | |

## 3.2. Longitudinal GM volume loss

The LME analyses testing the main effect of time on GM volume across all 122 regions in the atlas in patients identified five regions with significant volume loss according to the FWE-corrected threshold ($\alpha_{FWE}$ = 0.05/122 = 4.1 · $10^{-4}$). In particular, right (t = −6.9, p < $10^{-4}$) and left middle frontal gyrus (t = −5.8, p < $10^{-4}$), right cerebellum exterior (t = −5.7, p < $10^{-4}$), right superior parietal (t = −5.1, p < $10^{-4}$) and left superior frontal areas (t = −4.7, p = 1 · $10^{-4}$) were affected (Fig. 2). An evaluation of the interaction effect of time and group or the disease-specificity of the temporal dynamic of regional volume loss in these five regions respectively showed that atrophy in the right cerebellum exterior was significantly more pronounced in patients than controls (t = −2.9, p = 0.005).

## 3.3. Predicting future GM atrophy in MS based on perceived stress

Testing the association between perceived stress ratings (post-minus pre-stress) and longitudinal volume loss for the five regions subject to atrophy in pwMS showed that psychological insensitivity to stress was coupled to stronger longitudinal atrophy in the right superior parietal lobule. In other words, higher differential stress ratings were positively associated to the volume difference for T1 – T0 in this area (t = 3.1, p = 0.007).

## 3.4. Predicting future GM atrophy in MS based on neural stress responses

This analysis showed that differential stress activity of two networks predicted future GM loss in two of the five regions. In particular, following the FWE-corrected threshold ($\alpha_{FWE}$ = 0.05/25 = 0.002), stress-induced activity of the 18th network (comprising a variety of prefrontal brain areas) was negatively associated with atrophy (i.e., positively with the volume difference T1 – T0; t = 5.1, p = < $10^{-4}$) in right superior parietal lobule. Furthermore, the 22nd network including a variety of prefronto-limbic areas was positively linked to future volume loss in the right exterior cerebellum (i.e., negatively to the
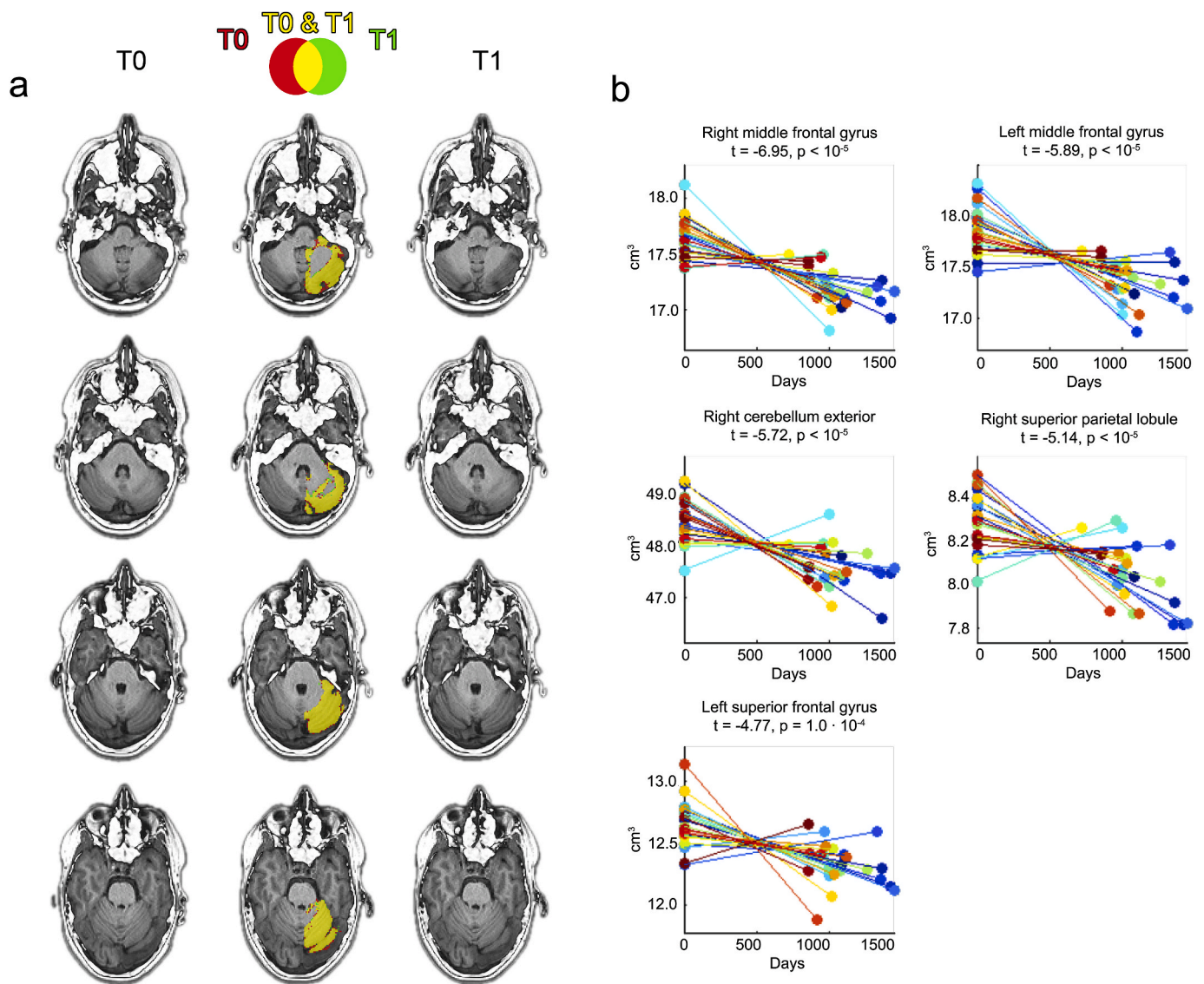


**Fig. 2. Longitudinal GM atrophy. (a)** On the left side, the computation of longitudinal GM volume variations is illustrated for an arbitrary person with multiple sclerosis and selected axial slices of the right exterior cerebellum. Specifically, superimposed on the native anatomical T1-weighted images of this patient, red (green) areas highlight voxels classified as right exterior cerebellum at T0 (T1) by the procedure used for volume computation in our analyses. Yellow areas were classified as right exterior cerebellum voxels at both time points. **(b)** Regions with significant longitudinal GM volume reductions across pwMS. In all subgraphs in (b), the regional volumes were corrected for covariates of no interest. (For interpretation of the references to colour in this figure legend, the reader is referred to the Web version of this article.)

difference T1 – T0; t = −4.4, p = 3 · 10⁻⁴; Fig. 3).

### 3.5. Perceived stress and neural stress responses in MS

This analysis showed that activity of one of the two networks predicting longitudinal atrophy was related to the difference of stress ratings for the post-minus pre-stress stage. Specifically, following the FWE-corrected significance threshold ($\alpha_{FWE} = 0.05/2 = 0.025$), activity of the 18th network was positively linked to psychological stress (t = 4.7, p = 5 · 10⁻⁴; Fig. 4).

### 4. Discussion

We investigated whether neurocognitive stress processing during exposure to mild psychological stress predicts future GM atrophy in persons with MS accumulated over a period of roughly 1000 days.

Four main analyses were conducted. In the first, we evaluated anatomical MRI data to identify GM regions affected by longitudinal atrophy in pwMS as targets for our predictive analyses and compared the patients' longitudinal atrophy to that of controls to evaluate its disease-specificity. We could show a significant loss in five regions, i.e., in both middle frontal gyri, left superior frontal gyrus, right superior parietal lobule and right cerebellum exterior. Moreover, we showed that atrophy in right cerebellum exterior was more pronounced in patients than controls and can thus be considered MS-specific. The spatiotemporal pattern of GM atrophy found in this study is in good accordance with findings of MS atrophy studies (e.g., Eshaghi et al., 2018; Pagani et al., 2005; Bendfeldt et al., 2009), especially when the difference in regional GM volume between patients and controls is considered independent of the impact of time (Fig. S2).
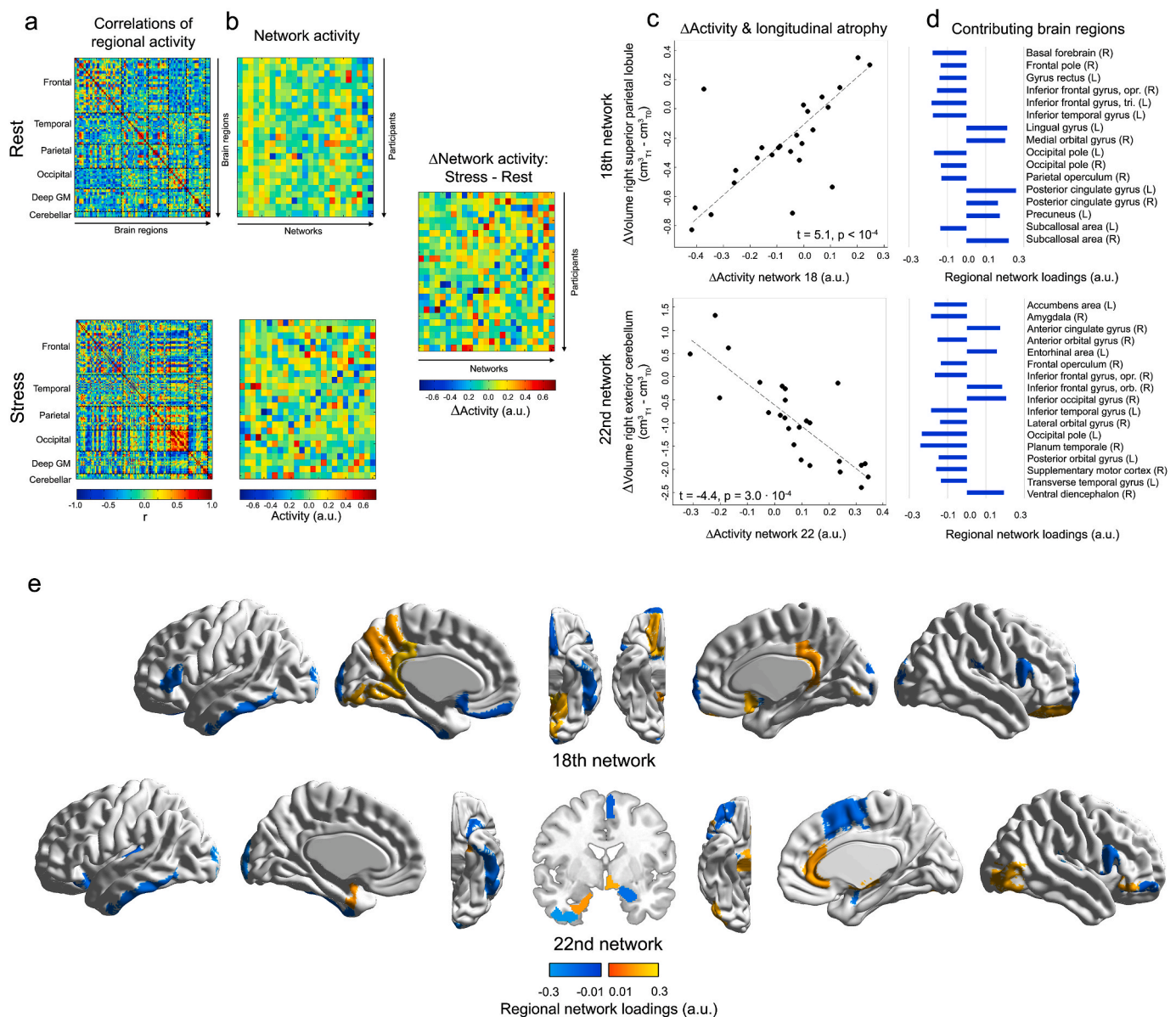


**Fig. 3. Neural network activity and future GM atrophy. (a)** Matrices showing the correlation of activity for the pairs of regions included in the neuroanatomical atlas separately for resting and stress stage. **(b)** Activity of neural stress networks during stress and resting stage and differential activity between these two conditions. **(c)** Significant association between differential stress activity of the 18th network and longitudinal GM volume loss in the right superior parietal lobule and between differential activity of the 22nd network and volume loss in the right cerebellum exterior. Longitudinal volume loss of both regions was corrected for covariates of no interest (see section 2.5.3 for details). **(d, e)** Brain regions included in the atlas with a significant link to the two networks as determined by a permutation test (see supplementary methods for details).
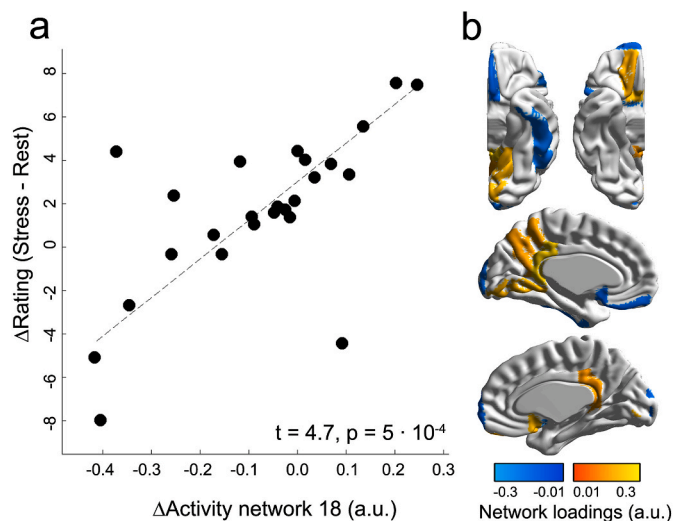
**Fig. 4. Neural network activity and perceived stress. (a)** The scatterplot on the left depicts the association between activity of the 18th network (also predictive of longitudinal GM atrophy of right superior parietal lobule) and the difference between the post- and the pre-stress stage (corrected for covariates of no interest). In **(b)** we again depict the brain regions contributing to (activity of) network 18 for better comprehensibility.

In the second analysis, we tested whether psychological stress predicts future atrophy in the five areas revealed by the first analysis and found that atrophy in right superior parietal lobule could be predicted. Importantly, stronger feelings of being stressed by the task were coupled to *less* future atrophy. This finding of a detrimental effect of psychological stress insensitivity for disease processes is compatible with a positive link between HPA-axis activity in pharmacological challenge tasks and future EDSS in pwMS (Gold et al., 2005; Kern et al., 2013). Additionally, it fits well to the negative cross-sectional link between stress-induced brain activity and clinical disability and atrophy found in pwMS in (Weygandt et al., 2016).

In the third analysis, we tested whether stress-induced neural network activity predicts future atrophy in the five GM areas identified in pwMS in the first analysis and found that activity of two networks (Wang et al., 2005; Wager et al., 2005) predicted regional GM volume loss of two GM areas. Together, (i) the specific areas contributing to both networks and (ii) the association between activity of the 18th network and salivary cortisol shown in the Supplement (although this should be interpreted carefully due to the small number of samples available in this supplementary analysis), these findings argue that glucocorticoids might contribute to the link between stress-induced brain activity and future MS atrophy. Specifically, activity of a network primarily consisting of prefrontal cortex areas was negatively related to longitudinal volume loss in the right superior parietal lobule. The areas contributing to this network are compatible with stress-sensitive prefronto-regions found in an fMRI stress study by Wang et al. (2005) and even more so with a study by (Urry et al., 2006) who showed a regulatory function of these areas for daytime cortisol release. Notably, this network also comprised the basal forebrain, a key area of the cholinergic systems (Paul et al., 2015) which can stimulate glucocorticoid release by the HPA axis (see below). Activity of the second network which primarily comprised limbic brain regions (i.e., amygdala, ventral diencephalon [which includes the hypothalamus], enthorinal cortex, anterior cingulate cortex, orbitofrontal gyri, and gyrus rectus) was negatively related to longitudinal volume loss in the right exterior cerebellum. Limbic areas are the key regulators of glucocorticoid release by the HPA axis (Urry et al., 2006).

Interestingly, a longitudinal association of glucocorticoid-related brain activity and GM loss is consistent with findings of cross-sectional studies in healthy subjects demonstrating a positive link between

cortisol release after dexamethasone application and ventricular volume (Schumann et al., 2002). Moreover, a contribution of the basal forebrain to atrophy predictive networks is also in line with a glucocorticoid-related explanation of MS atrophy as stress-induced choline release in this area can subsequently stimulate the HPA axis (Paul et al., 2015).

Several studies have proposed explanations for mechanisms underlying stress and glucocorticoid mediated neurodegeneration. Specifically, animal studies showed that chronic stress leads to permanent loss of dendrites in the rat prefrontal cortex (Radley et al., 2006) and that sustained and excessive glucocorticoid release in mice provokes increased loss of stable dendritic spines developed early in life (Liston and Gan, 2011). Thus, considering that the GM signal measured with T1-weighted MRI sequences does not solely account for cell bodies but also dendrites (Zatorre et al., 2012), dendritic loss induced by excess glucocorticoid availability (common in MS; Michelson et al., 1994) could be a predictable measure of GM loss in MS in this study.

Finally, in the fourth analysis, we tested the association between atrophy-predictive network activity and psychological stress and found that network activity predictive of right superior parietal lobule atrophy was positively related to perceived stress. Together, the findings that psychological (second analysis) and neural stress processing (third analysis) were negatively related to atrophy of this area and that they showed a positive mutual correlation (this analysis) strengthen our above interpretation that blunted neurocognitive stress processing has a detrimental effect on the course of MS. Please note that this presumably also holds for the link between limbic network activity and cerebellar atrophy – at least if one takes i. the negative link of amygdala CBF and activity of this network (Fig. 3d) and ii. the positive link of the network's activity and atrophy as guiding principle since amygdala activity is positively linked to cortisol release (Urry et al., 2006).

Importantly, blunted affective processing in MS has been reported by several other studies. For example Kleeberg et al. (2004), showed with a decision-making task that necessitates the perception of learned emotional arousal preceding (and putatively preventing) a negative choice that this affective learning process (i.e., an increase of anticipatory skin conductance during poor options) was much weaker in patients than controls. Consistently, we could show using an fMRI version of this task that activity in ventromedial prefrontal/orbitofrontal areas (i.e., the regions coding for and regulating these so-called somatic-markers) was positively linked to the task performance of pwMS and HCs. Simultaneously both parameters, performance and activity, were lower in patients (Weygandt et al., 2018).

Several aspects of the study warrant further discussions. The fact that the joint availability of fMRI stress data acquired at T0 and longitudinal GM volume data covering T0 and T1 was only given for pwMS is a major limitation of this work as this complicates an assessment of whether stress-based predictability of longitudinal atrophy is MS-specific or rather a more global, generic phenomenon. Consequently, we conducted two steps/analyses to address this potential weakness. First, we tested in the second subanalysis included in '2.5.1 Analysis of longitudinal GM volume loss' whether the volume loss of areas identified in the MS-specific first subanalysis of 2.5.1 was more pronounced in MS than the sMRI control group and thus whether longitudinal volume loss had an MS-specific dynamic in these regions. This revealed that this was the case for the right exterior cerebellum. Second, we conducted a supplementary analysis of stress network activity differences between patients and controls based on the fMRI data of pwMS and the fMRI control group. This showed that none of the two neural networks predictive of atrophy in pwMS was characterized by hyper- or hypoactivity in pwMS compared to HCs. Together, these findings suggest that future regional volume loss (partially) specific for MS (i.e., in exterior cerebellum) is preceded by specific patterns of stress-evoked activity in MS but that it is not the activity that directly drives volume loss but that (unknown) additional MS-specific factors linked to stress-evoked brain activity heighten the vulnerability of neural tissue to processes regulated by/

attached to this activity in MS.

Another point necessitating further notice is the difference in stress responses across measures evaluated. Except for one marker, each parameter (i.e., heart rate, subjective stress ratings, and neural networks comprising key stress processing regions) indicated a clear stress response. However, it should be noted that the task did not elicit a pronounced HPA response. This finding might be explained by two factors. First, it is known that stress tasks without a strong social evaluative component (e.g., without public speaking) sometimes fail to elicit such a response (see Michelson et al. (1994) for an overview) and even when a strong evaluative component is included, a marked HPA response is not guaranteed (Dimitrov et al., 2018). Second, results of Dimitrov et al. (2018) and Muehlhan et al. (2011) suggest that an MRI session can act as a potent stressor/trigger for cortisol release independent of the stimuli applied and that this stressor can trigger a maximal cortisol release at session onset which is followed by a continuous decline across the session – which exactly describes the cortisol trajectories observed here. Consequently, it is possible that the cortisol release triggered by MRI scanning onset concealed a weaker task-induced cortisol response.

A final aspect that should be critically discussed is that of potential confounding factors that might drive the link between neural stress processing and future atrophy. In line with findings of Kennedy and Scholey (2000) showing that inter-participant response differences in typical stress measures during a mental arithmetic task such as heart rate might simply reflect differences in functioning of a cardiac mechanism aiming to adopt brain glucose delivery to differences in cognitive effort/metabolic demands, variations in task load might be a factor coming into one's mind at this point. However, given that all analyses in this work relying on functional stress-response measures (2.5.2, 2.5.3, 2.5.4, and the supplementary analysis of psychophysiological stress task responses) included task load as covariate of no interest in the respective linear regression models to capture the impact of this factors, this possibility appears highly unlikely. Other conceivable confounding factors might comprise alternative MS-related mechanisms. Again, however, this appears unlikely in the context of this work. Firstly, development of new brain lesions in a time period of one year prior to fMRI scanning (i. e., stress-induction at T0) was very restricted in fifteen MS patients for which corresponding T2-weighted images were available for evaluation (cf. Supplement). Secondly, the median number of days between last relapse and T0 across all patients was 657 days. Thirdly, voxel coordinates containing lesions at T0 were not evaluated in computation of neural network activity. Fourthly, volume of each GM region at T0 was included as covariate of no interest in analyses modelling atrophy between T0 and T1 for that region. Together, these factors suggest that potential alternative MS-related mechanisms did not have an essential impact on the association between neural stress network activity at T0 and future GM atrophy.

In conclusion, when considering that neural (Sinha et al., 2016) and psychological (Mohr et al., 2012) stress processing can be modified through cognitive interventions, and given the relevance of parietal (Sepulcre et al., 2009; Hanken et al., 2016) and cerebellar (Cocozza et al., 2017; D'Ambrosio et al., 2017) pathology for MS, stress processing might constitute a modifiable disease factor of high clinical importance.

## CRediT authorship contribution statement

**Lil Meyer-Arndt:** Conceptualization, Investigation, Writing - original draft, Writing - review & editing. **Stefan Hetzer:** Software, Writing - original draft, Writing - review & editing. **Susanna Asseyer:** Investigation, Writing - original draft, Writing - review & editing. **Judith Bellmann-Strobl:** Investigation, Writing - original draft, Writing - review & editing. **Michael Scheel:** Investigation, Writing - original draft, Writing - review & editing. **Jan-Patrick Stellmann:** Writing - original draft, Writing - review & editing. **Christoph Heesen:** Writing - original draft, Writing - review & editing. **Andreas K. Engel:** Writing - original draft, Writing - review & editing. **Alexander U. Brandt:** Writing - original draft, Writing - review & editing. **John-Dylan Haynes:** Writing - original draft, Writing - review & editing. **Friedemann Paul:** Conceptualization, Writing - original draft, Writing - review & editing. **Stefan M. Gold:** Conceptualization, Writing - original draft, Writing - review & editing. **Martin Weygandt:** Conceptualization, Methodology, Software, Validation, Formal analysis, Investigation, Writing - original draft, Writing - review & editing, Visualization.

## Declaration of competing interest

None of the authors (Lil Meyer-Arndt, Stefan Hetzer, Susanna Asseyer, Judith Bellmann-Strobl, Michael Scheel, Jan-Patrick Stellmann, Christoph Heesen, Andreas K. Engel, Alexander U. Brandt, John-Dylan Haynes, Friedemann Paul, Stefan M. Gold, and Martin Weygandt) has a competing interest in the context of this work.

## Appendix A. Supplementary data

Supplementary data to this article can be found online at https://doi.org/10.1016/j.ynstr.2020.100244.

## References

Bendfeldt, K., Kuster, P., Traud, S., Egger, H., Winklhofer, S., Mueller-Lenke, N., et al., 2009. Association of regional gray matter volume loss and progression of white matter lesions in multiple sclerosis - a longitudinal voxel-based morphometry study. Neuroimage 45, 60–67.

Charcot, Jean-Martin, 1877. Lectures on Diseases of the Nervous System. New Sydenham Society. London.

Cocozza, S., Petracca, M., Mormina, E., Buyukturkoglu, K., Podranski, K., Heinig, M.M., et al., 2017. Cerebellar lobule atrophy and disability in progressive MS. J. Neurol. Neurosurg. Psychiatry 88, 1065–1072.

Compston, A., Coles, A., 2008. Multiple sclerosis. Lancet 372, 1502–1517.

Confavreux, C., Vukusic, S., 2006. Accumulation of irreversible disability in multiple sclerosis: from epidemiology to treatment. Clin. Neurol. Neurosurg. 108, 327–332.

D'Ambrosio, A., Pagani, E., Riccitelli, G.C., Colombo, B., Rodegher, M., Falini, A., et al., 2017. Cerebellar contribution to motor and cognitive performance in multiple sclerosis: an MRI sub-regional volumetric analysis. Mult. Scler. 23, 1194–1203.

Dimitrov, A, Demin, K, Fehlner, P, Walter, H, Erk, S, Veer, I-M, 2018. Differences in neural recovery from acute stress between cortisol responders and non-responders. Front. Psychiatr. 9, 631.

Eshaghi, A., Marinescu, R.V., Young, A.L., Firth, N.C., Prados, F., Jorge Cardoso, M., et al., 2018. Progression of regional grey matter atrophy in multiple sclerosis. Brain 141, 1665–1677, 2018.

Fox, J., Weisberg, S., 2019. An R Companion to Applied Regression, third ed. Sage, Thousand Oaks, CA.

Geurts, J.J., Calabrese, M., Fisher, E., Rudick, R.A., 2012. Measurement and clinical effect of grey matter pathology in multiple sclerosis. Lancet Neurol. 11, 1082–1092.

Golan, D., Somer, E., Dishon, S., Cuzin-Disegni, L., Miller, A., 2008. Impact of exposure to war stress on exacerbations of multiple sclerosis. Ann. Neurol. 64, 143–148.

Gold, S.M., Raji, A., Huitinga, I., Wiedemann, K., Schulz, K.H., Heesen, C., 2005. Hypothalamo-pituitary-adrenal axis activity predicts disease progression in multiple sclerosis. J. Neuroimmunol. 165, 186–191.

Good, P., 2005. Permutation, Parametric and Bootstrap Tests of Hypotheses, third ed. Springer. New York.

Hanken, K., Bosse, M., Möhrke, K., Eling, P., Kastrup, A., Antal, A., Hildebrandt, H., 2016. Counteracting fatigue in multiple sclerosis with right parietal anodal transcranial direct current stimulation. Front. Neurol. 7, 154. eCollection.

Kalincik, T., 2017. Stop inflammation and you stop neurodegeneration in MS – NO. Mult. Scler. 23, 1321–1323.

Kennedy, D.O., Scholey, A.B., 2000. Glucose administration, heart rate and cognitive performance: effects of increasing mental effort. Psychopharmacology (Berlin) 149 (1), 63–71.

Kern, S., Krause, I., Horntrich, A., Thomas, K., Aderhold, J., Ziemssen, T., 2013. Cortisol awakening response is linked to disease course and progression in multiple sclerosis. PloS One 8, e60647.

Kleeberg, J., Bruggimann, L., Annoni, J.M., van Melle, G., Bogousslavsky, J., Schluep, M., 2004. Altered decision-making in multiple sclerosis: a sign of impaired emotional reactivity? Ann. Neurol. 56, 787–795.

Kurtzke, J.F., 1983. Rating neurologic impairment in multiple sclerosis: an expanded disability status scale (EDSS). Neurology 33, 1444–1452.

Liston, C., Gan, W.B., 2011. Glucocorticoids are critical regulators of dendritic spine development and plasticity in vivo. Proc. Natl. Acad. Sci. U. S. A. 108, 16074–16079.

Michelson, D., Stone, L., Galliven, E., Magiakou, M.A., Chrousos, G.P., Sternberg, E.M., et al., 1994. Multiple sclerosis is associated with alterations in hypothalamic-pituitary-adrenal axis function. J. Clin. Endocrinol. Metab. 79, 848–853.

Mohr, D.C., Hart, S.L., Julian, L., Cox, D., Pelletier, D., 2004. Association between stressful life events and exacerbation of multiple sclerosis: a meta-analysis. BMJ 328, 731.

Mohr, D.C., Lovera, J., Brown, T., Cohen, B., Neylan, T., Henry, R., et al., 2012. A randomized trial of stress management for the prevention of new brain lesions in MS. Neurology 79, 412–419.

Muehlhan, M., Lueken, U., Wittchen, H.-U., Kirschbaum, C., 2011. The scanner as a stressor: evidence from subjective and neuroendocrine stress parameters in the time course of a functional magnetic resonance imaging session. Int. J. Psychophysiol. 79 (2), 118–126.

Pagani, E., Rocca, M.A., Gallo, A., Rovaris, M., Martinelli, V., Comi, G., et al., 2005. Regional brain atrophy evolves differently in patients with multiple sclerosis according to clinical phenotype. Am. J. Neuroradiol. 26, 341–346.

Paul, S., Jeon, W.K., Bizon, J.L., Han, J.S., 2015. Interaction of basal forebrain cholinergic neurons with the glucocorticoid system in stress regulation and cognitive impairment. Front. Aging Neurosci. 7, 43.

Radley, J.J., Rocher, A.B., Miller, M., Janssen, W.G., Liston, C., Hof, P.R., et al., 2006. Repeated stress induces dendritic spine loss in the rat medial prefrontal cortex. Cerebr. Cortex 16, 313–320.

Reich, D.S., Lucchinetti, C.F., Calabresi, P.A., 2018. Multiple sclerosis. N. Engl. J. Med. 378, 169–180.

Schumann, E.M., Kumpfel, T., Then Bergh, F., Trenkwalder, C., Holsboer, F., Auer, D.P., 2002. Activity of the hypothalamic-pituitary-adrenal axis in multiple sclerosis: correlations with gadolinium-enhancing lesions and ventricular volume. Ann. Neurol. 51, 763–767.

Sepulcre, J., Masdeu, J.C., Goñi, J., Arrondo, G., Vélez de Mendizábal, N., Bejarano, B., Villoslada, P., 2009. Fatigue in multiple sclerosis is associated with the disruption of frontal and parietal pathways. Mult. Scler. 15, 337–344.

Sinha, R., Lacadie, C.M., Constable, R.T., Seo, D., 2016. Dynamic neural activity during stress signals resilient coping. Proc. Natl. Acad. Sci. U. S. A. 113, 8837–8842.

Song, H., Fang, F., Tomasson, G., Arnberg, F.K., Mataix-Cols, D., Fernández de la Cruz, L., et al., 2018. Association of stress-related disorders with subsequent autoimmune disease. J. Am. Med. Assoc. 319, 2388–2400.

Thompson AJ, Banwell BL, Barkhof F, Carroll WM, Coetzee T, Comi G, et al. Diagnosis of multiple sclerosis: 2017 revisions of the McDonald criteria. Lancet Neurol. 17: 162-173.

Urry, H.L., van Reekum, C.M., Johnstone, T., Kalin, N.H., Thurow, M.E., Schaefer, H.S., et al., 2006. Amygdala and ventromedial prefrontal cortex are inversely coupled during regulation of negative affect and predict the diurnal pattern of cortisol secretion among older adults. J. Neurosci. 26, 4415–4425.

Wager, T.D., Keller, M.C., Lacey, S.C., Jonides, J., 2005. Increased sensitivity in neuroimaging analyses using robust regression. Neuroimage 26, 99–113.

Wang, J., Rao, H., Wetmore, G.S., Furlan, P.M., Korczykowski, M., Dinges, D.F., Detre, J. A., 2005. Perfusion functional MRI reveals cerebral blood flow pattern under psychological stress. Proc. Natl. Acad. Sci. U. S. A. 102, 17804–17809.

Weygandt, M., Meyer-Arndt, L., Behrens, J.R., Wakonig, K., Bellmann-Strobl, J., Ritter, K., et al., 2016. Stress-induced brain activity, brain atrophy, and clinical disability in multiple sclerosis. Proc. Natl. Acad. Sci. U. S. A. 113, 3444–3449.

Weygandt, M., Wakonig, K., Behrens, J., Meyer-Arndt, L., Soeder, E., Brandt, A.U., et al., 2018. Brain activity, regional gray matter loss, and decision-making in multiple sclerosis. Mult. Scler. 24, 1163–1173.

Weygandt, M., Spranger, J., Leupelt, V., Maurer, L., Bobbert, T., Mai, K., et al., 2019. Interactions between neural decision-making circuits predict long-term dietary treatment success in obesity. Neuroimage 184, 520–534.

Zatorre, R.J., Fields, R.D., Johansen-Berg, H., 2012. Plasticity in gray and white: neuroimaging changes in brain structure during learning. Nat. Neurosci. 15, 528–536.